Journal of Molecular Catalysis A: Chemical 310 (2009) 1–8

Contents lists available at ScienceDirect

Journal of Molecular Catalysis A: Chemical

journal homepage: www.elsevier.com/locate/molcata

Mesoporous Ga-MCM-41 as support for metallocene catalysts: Acidity–activity relationship

João M. Campos[a], João Paulo Lourenço[b], Auguste Fernandes[c], Ana Maria Rego[d], M. Rosário Ribeiro[a,*]

[a] Instituto de Ciência e Engenharia de Materiais e Superfícies (ICEMS), Departamento de Engenharia Química e Biológica, Instituto Superior Técnico - Universidade Técnica de Lisboa, Av. Rovisco Pais, 1049-001 Lisboa, Portugal
[b] Centro de Investigação em Química do Algarve (CIQA), Departamento de Química, Bioquímica e Farmácia, Faculdade de Ciências e Tecnologia, Universidade do Algarve, Faro, Portugal
[c] Instituto de Biotecnologia e Bioengenharia (IBB), Departamento de Engenharia Química e Biológica, Instituto Superior Técnico - Universidade Técnica de Lisboa, Lisboa, Portugal
[d] Centro de Química-Física Molecular (CQFM) and Institute of Nanoscience and Nanotechnology (IN), Departamento de Engenharia Química e Biológica, Instituto Superior Técnico - Universidade Técnica de Lisboa, Lisboa, Portugal

ARTICLE INFO

Article history:
Received 25 February 2009
Received in revised form 12 May 2009
Accepted 14 May 2009
Available online 22 May 2009

Keywords:
Metallocenes
Ethylene
Polymerisation
MCM-41
Acidity

ABSTRACT

Several Ga-MCM-41 materials, prepared using different synthesis and template removal procedures, were used for the immobilisation of Cp_2ZrCl_2 by a direct impregnation method. Supports were carefully characterised by XRD, N_2 adsorption, ICP-AES, AAS, XPS and FTIR (using pyridine as probe molecule for acid sites), in order to assess their structural features, chemical composition (bulk and surface) and surface acidity properties.

Supported catalysts were tested for the polymerisation of ethylene, using methylaluminoxane (MAO) as cocatalyst/activator. The relationships established between concentration/strength of acid sites of Ga-MCM-41 and the catalytic performance of zirconocene dichloride supported in these materials demonstrate that the behaviour of the catalytic systems analysed in this paper is compatible with existing models for the interaction of single-site olefin polymerisation catalysts with other inorganic acidic oxides.

1. Introduction

The activity of metallocenes and similar single-site catalysts olefin polymerisation catalysts is known to depend on a multitude of factors related to the nature of activator–catalyst–monomer interactions. Heterogenisation of some of these components, aiming at a better control of polymer morphologies, brought additional levels of complexity to the study of the catalytic system, due to additional interactions with the support. Mesoporous silicates of the MCM-41 family are one of the many types of inorganic materials being investigated as supports for olefin polymerisation catalysts [1–7]. These materials present structures with nanoscale-organised one-dimensional mesopores deemed responsible for the unusual morphologies and mechanical properties sometimes observed in the resulting polyolefins [8,9]. Mesoporous silicates also present high potential in the preparation of hybrid organic–inorganic nanocomposites by *in situ* polymerisation of olefins [10–13], where they act as nanofillers.

Moreover, mesoporous silicates are also known to allow an easy modification of their acidic surface properties. The most frequently used pathway to achieve that is by incorporation of aluminium atoms in their structures, although boron and some transition metals such as Zn, Ti and Fe may also be employed. The nature of the element introduced, together with its content (Si/element atomic ratio) will determine the acid site distribution (i.e. the number and strength of Lewis and Brønsted sites) [14,15]. Some authors have already pointed out the determinant role that surface acidity properties of solid supports may play in the activation of the metallocene catalyst and, consequently, on the corresponding polymerisation activity [16–19].

So far, few research groups have directly characterised the surface acidity of mesoporous materials and related it with the performance of metallocene catalysts immobilised in their surfaces [20–24].

Recently, we reported the use of Ga-MCM-41 as support for metallocene catalysts. It was shown that the resulting supported Cp_2ZrCl_2 catalysts ($Cp = \eta^5\text{-}C_5H_5$), prepared by a direct impregnation method, presented high activities for ethylene polymerisation, and it was suggested that the acidity derived from the introduction of Ga in the mesoporous silicate support would play an important role on the formation of the active species and on the resulting polymerisation activity [25]. In the present work, several mesoporous gallosilicates, prepared by two main methods (direct synthesis and post-synthesis treatment), are extensively characterised to assess

* Corresponding author. Tel.: +351 218417325; fax: +351 218419198.
E-mail address: rosario@ist.utl.pt (M.R. Ribeiro).

1381-1169/$ – see front matter © 2009 Elsevier B.V. All rights reserved.
doi:10.1016/j.molcata.2009.05.012

their structural features, chemical composition (bulk and surface) and surface acidity and correlate these properties with the ethylene polymerisation behaviour.

2. Experimental

2.1. Synthesis of MCM-41 materials containing gallium (Ga-MCM-41)

Purely siliceous MCM-41 (Si-MCM-41) was prepared according to the method described by Kim et al. [26]. Ga-MCM-41 supports, with different Si/Ga ratios (samples GaM*R*, where *R* stands for the Si/Ga ratio), were prepared by a direct synthesis method adapted from the synthesis of AlMCM-41 described by Lindlar et al. [27]. The metal source in this case was $Ga(NO_3)_3$. The template was partially removed by extraction with a 0.1 M NH_4NO_3 in 96% ethanol at reflux for 2 h. After drying, the products were calcined under a flow of dry air at 550 °C for 12 h. Selected samples were extracted twice with the alcoholic solution of NH_4NO_3 and calcined under a flow of dry air at 550 °C for 24 h (samples GaM*R*X).

The procedure for the preparation of Ga-MCM-41 by a post-synthesis treatment (samples GaM*R*I) was adapted from the method described by Lang et al. for the incorporation of other metals [28]. In a typical procedure, 2 g of as-synthesized Si-MCM-41 were dispersed in a solution containing 160 mL H_2O and the required amount of $Ga(NO_3)_3$. The mixture was stirred at room temperature for 1 h followed by 20 h at 80 °C. After recovering and drying at 80 °C, the template was removed by the same procedure described above for the samples GaM*R*.

2.2. Characterisation of Ga-MCM-41 materials

All the samples prepared were checked for phase identification by powder X-ray diffraction on a Panalitycal X'Pert Pro diffractometer using Cu Kα radiation filtered by Ni and a X'Celerator detector. Nitrogen adsorption isotherms were obtained at −196 °C in an ASAP 2010 Micromeritics equipment. Prior to the measurements, the samples were degassed at 350 °C for 3 h.

The bulk compositions of the various materials prepared were determined using a combination of AAS and ICP-AES techniques.

Surface chemical analysis was performed by XPS in an XSAM800 spectrometer (Kratos) operated in Fixed Analyzer Transmission (FAT) mode, with a pass energy of 20 eV and the non-monochromatised Mg Kα and Al Kα X-radiation ($h\upsilon$ = 1253.7 and 1486.7 eV, respectively). Power was 120 W (12 kV × 10 mA). Samples were mounted on a double-face tape and analysed in an ultra-high-vacuum chamber (~10^{-7} Pa) at room temperature. Spectra were recorded by a Sun SPARC Station 4 with Vision software (Kratos) using a step of 0.1 eV. A Shirley background was used for baseline subtraction and curve fitting for component peaks was carried out with Gaussian–Lorentzian products. No flood-gun was used for charge compensation. Binding energies were corrected relative to C 1s (binding energy = 285 eV) from carbonaceous contamination [29]. X-ray source satellites were subtracted. For quantification purposes, sensitivity factors were 0.66 for O 1s, 0.25 for C 1s, 4.74 for Ga $2p_{3/2}$ and 0.27 for Si 2p.

The acid sites of the different mesoporous gallosilicates were characterised by FTIR, using pyridine as probe molecule. Self-supported wafers (5–10 mg) were placed in an IR quartz cell and then evacuated under secondary vacuum (10^{-6} Torr) at 300 °C for 1 h, prior to pyridine adsorption at room temperature (equilibrium pressure ~1 Torr). Subsequent desorption of pyridine was performed at 150 and 300 °C under secondary vacuum. IR spectra were recorded on a Thermo Nicolet Nexus instrument (64 scans with a resolution of 4 cm^{-1}). The background spectrum, recorded under identical operating conditions, was automatically subtracted from each sample spectrum. In order to obtain a quantitative measurement of the acidity of the materials, the amounts of pyridine adsorbed for each type of acid site were calculated using extinction molar coefficients from Emeis [30].

2.3. Preparation of the supported catalysts and ethylene polymerisations

Full accounts of the procedure followed in the preparation of the catalyst, as well as the polymerisation setup and methods, were already published [31]. In this paper, a brief description of these procedures will be given.

A direct impregnation method was used for the immobilization of zirconocene dichloride (Cp_2ZrCl_2, Cp = η^5-C_5H_5, Aldrich) in the Ga-MCM-41 supports. Prior to use, the mesoporous solids are heated at 5 °C/min up to 300 °C, with nitrogen purging, and kept at this temperature for 2 h. The method used for the preparation of the supported catalysts is described in a previous paper [31]. In this method, the support is contacted for 16 h, at room temperature, with a dilute metallocene solution, in such a concentration (1.7×10^{-3} M) that all metallocene is adsorbed. Therefore the concentration of Zr in the solid is determined from stoichiometric calculations. The quantitative adsorption of the metallocene is confirmed using the following procedure: after contacting the Cp_2ZrCl_2 solution with the support, the catalyst slurry is decanted and the remaining solution is injected in the polymerisation reactor, and MAO is added. No polyethylene is formed from this solution, thus confirming that the adsorption of the metallocene by the solid was complete. This way, a large set of Ga-MCM-41-supported catalysts were obtained in the form of identical suspensions (34 mg solid/mL) with constant Cp_2ZrCl_2 loads (50 μmol Zr/g solid), and subsequently tested under identical polymerisation conditions.

Polymerisations were carried out in a glass reactor, using toluene as solvent, at 25 °C and ethylene monomer at 1.2 bar abs. After loading the solvent and saturating it with ethylene, an adequate amount of MAO cocatalyst was added (such that Al/Zr ~ 500 or Al/Zr ~ 1500), and the supported catalyst suspension was injected to the reactor (~1 mL = 2 μmol Zr). The total volume in the reactor was matched to 50 mL. The reaction time in these polymerisations was set to 30 min, after which the polymer was quickly precipitated over a mixture of methanol and HCl (5%). Polymer was thoroughly washed twice, with fresh methanol, before drying and weighting. For each supported catalyst polymerisation tests were repeated 2–3 times under the same experimental conditions, in order to check reproducibility. Activity values correspond to the average of the independent experiments.

Some additional exploratory experiments were also performed, using TIBA (Aldrich) in place of MAO. In these cases the Al/Zr ratio used was 50:1 and the reaction time was 120 min.

3. Results and discussion

3.1. Synthesis and structural characterisation of Ga-MCM-41 materials

The incorporation of Ga into the structure of MCM-41 by direct synthesis causes a broadening of the peaks in the XRD pattern characteristic of the hexagonal symmetry, when compared with the pure siliceous counterpart, a result already observed for the incorporation of Al [14,31]. Nevertheless, as shown in Fig. 1 for GaM82, the hexagonal structure of the Ga-containing materials is clearly identified by the three diffraction peaks that can be indexed as (1 0 0), (1 1 0) and (2 0 0) in this symmetry. The more severe conditions used for the template removal did not have a significant

Table 1
The mesoporous solids prepared and their structural characteristics.

Sample type	Sample designation	Bulk Si/Ga	a_0 (Å)[a]	S_{BET} (m^2/g)	V_p (cm^3/g)[b]	D_p (Å)[c]
Si-MCM-41	MSI	∞	48.7	1007	0.850	33.8
Ga-MCM-41 by direct synthesis	GaM139	139	47.8	868	0.699	32.2
	GaM116	116	49.4	841	0.704	33.5
	GaM82	82	50.3	1016	0.890	35.0
	GaM63	63	49.5	734	0.628	34.2
	GaM47	47	51.5	800	0.688	34.4
	GaM82X[d]	82	48.2	1020	0.872	34.2
	GaM63X[d]	63	47.8	847	0.720	34.0
	GaM47X[d]	47	49.3	859	0.745	34.7
Ga-MCM-41 by impregnation of Si-MCM-41	GaM150I	150	47.0	977	0.826	33.8
	GaM126I	126	47.8	1085	0.875	32.3
	GaM83I	83	47.3	964	0.764	31.7

[a] Calculated for a hexagonal symmetry as $a_0 = 2d_{100}/3^{1/2}$.
[b] Calculated at the top of the adsorption step.
[c] $D_p = (4\,V_p/S_{BET})$.
[d] Extended treatment for template removal.

influence on the structural integrity of these samples. In fact the XRD patterns of the samples GaM82 and GaM82X are very similar. The sample Ga83I, prepared by a post-synthesis method reveals a diffraction pattern closely matching the one of Si-MCM-41 precursor. This was expected and shows that the technique used for the deposition of Ga over the surface of a pre-formed mesoporous material did not change its framework structure. It is important to note that the XRD patterns of the other Ga-containing samples (not shown in Fig. 1) display the same behaviour.

In order to check the formation of aggregates of Ga oxide or other Ga phases during the synthesis or the calcination procedures, a diffraction pattern was recorded in the 2θ range from 1.5° to 80°, for all samples. Diffraction peaks due to the presence of Ga crystalline phases were not detected. This indicates, even for the samples with low Si/Ga ratio, that the distribution of Ga is rather homogeneous or at least that the aggregates formed do not have a significant size to be detected by XRD.

Structural parameters, after template removal, calculated for the mesoporous materials from XRD and nitrogen adsorption data are presented in Table 1. The various samples are identified according to the procedure used in their synthesis and to their bulk Si/Ga ratios obtained from elemental analysis. Adsorption of nitrogen clearly shows that all samples have a high surface area and a rather similar pore diameter, in the range 31.7–35.0 Å. The extended calcination procedure carried out on the samples prepared by direct synthesis, caused, as expected, just a small contraction of the hexagonal unit cell but did not change significantly the structural parameters as observed by XRD and nitrogen adsorption data (series GaM*R* and GaM*R*X). Adsorption data of series GaM*R*I indicate, in line with the XRD measurements, that the technique used for the deposition of Ga on the surface of MCM-41 did not have significant influence on the structural parameters of the parent material. Just a small reduction in the pore diameter is observed for the sample with the highest amount of Ga.

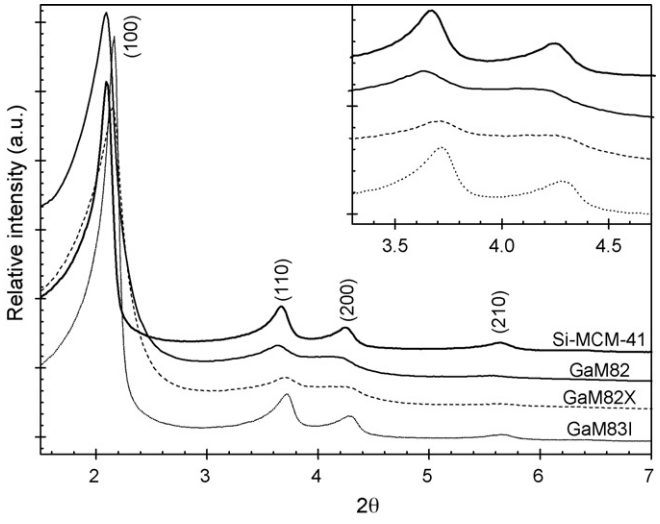

Fig. 1. XRD patterns obtained for the purely siliceous MCM-41 and for three Ga-MCM-41 materials with identical Ga loadings, prepared according to the methods presented in the current paper.

3.2. XPS analysis of Ga-MCM-41 materials

The various Ga-MCM-41 materials were surveyed by XPS. While elemental analysis affords the bulk Si/Ga ratio, XPS provides information regarding surface compositions. For porous, powdered materials, since the surface is not flat no information can be obtained about in-depth elemental composition by angle resolved XPS analysis. Instead, two different anodes, Al and Mg, were used, the former with higher radiation source energies than the latter. Since the escape depth of photoelectrons is a function of their kinetic energy, and it is higher when the source radiation has a higher energy, the information brought by photoelectrons generated by Al anode radiation comes from deeper thickness than when they are generated by Mg anode radiation. This way, shallower and deeper Si/Ga ratios were calculated for various Ga-MCM-41 samples, giving an idea of the depth distribution of gallium atoms in the surface of the solid. For Ga 2p photoelectrons, for instance, the escape depths are 0.64 and 1.37 nm in the case of Mg and Al anode, respectively. For the greater part of the samples, the Si/Ga ratio obtained with Al anode is larger than the one obtained with Mg anode, suggesting that gallium segregation exists at the external surface when compared with the region underneath, but still of the order of magnitude of 1 nm. However, for the same samples, Si/Ga ratios for both Al and Ga anodes are larger than those obtained by elemental analysis for the bulk material. These results are consistent with an intermediary zone of gallium depletion near the surface and a gallium enriched nucleus in the samples with lower gallium contents.

The three Si/Ga ratios become the same, within the experimental error, for samples with higher Ga loadings. The exception to this pattern is the sample GaM82, where a large segregation of gallium at the outer surface exists, confirmed by the smaller XPS Si/Ga ratios obtained with both anodes, when compared to the bulk elemental analysis. This sample also exhibits structural differences when

Table 2
Results of surface chemical analysis by XPS.

Sample type	Sample	Bulk Si/Ga	Si/Ga inner (Al anode)	Si/Ga outer(Mg anode)
Ga-MCM-41 by direct synthesis	GaM139	139	n.d.	n.d.
	GaM116	116	268	143
	GaM82	82	47	37
	GaM63	63	130	90
	GaM47	47	44	50
	GaM82X[a]	82	51	72
	GaM63X[a]	63	107	103
	GaM47X[a]	47	n.d.	n.d.
Ga-MCM-41 by impregnation of Si-MCM-41	GaM150I	150	21	19
	GaM126I	126	17	15
	GaM83I	83	14	11

n.d.: not determined.
[a] Extended treatment for template removal.

compared with the remaining samples (Table 1). It is interesting to notice that after preparing the same material using a longer calcination treatment (sample Ga82X), there is a decrease in the amount of gallium in its surface, particularly in the outer layers (Mg anode ratio). This suggests that a migration of gallium towards the particle nucleus occurred. In the sample GaM63, the same treatment induces a gallium homogenisation in the surface decreasing its amount in the outer layers but causing the depletion zone to disappear.

On the other hand, XPS data for the materials prepared by impregnation showed the lowest surface Si/Ga ratios of the entire set of samples. This is not surprising, as the impregnation technique will deposit and concentrate gallium over a thin layer in the surfaces of the Si-MCM-41, and not disperse it inside the siliceous framework, as it would happen if a gallium source had been added to the synthesis gel prior to crystallisation.

3.3. Surface acidity

The acidity of the Ga-MCM-41 materials was determined by adsorption of pyridine (probe molecule) at room temperature and subsequent desorption at 150 and 300 °C. The quantitative results are presented in Table 4. The amount of pyridine obtained at 150 °C corresponds to total acid sites, while that observed at 300 °C corresponds to medium–strong acid sites. For simplicity, weak (150 °C) and strong (300 °C) acid sites will be considered hereafter. Fig. 2 shows the typical FTIR spectra (before and after pyridine adsorption) obtained for GaMCM-41 samples (in this case GaM47X) and consequently the difference spectrum. Bands at 1457 and 1621 cm^{-1}, attributed to Lewis acid centres, are observed together with bands at 1545 and 1640 cm^{-1}, usually assigned to Brønsted acid sites [14,32] Band at 1491 cm^{-1} corresponds to both acid sites. Pure Si-MCM-41 does not show either Lewis or Brønsted acidity. For both the samples, the amount of Brønsted acid sites is very low, suggesting a low concentration of this type of acid sites in the mesoporous gallosilicates prepared. In all the cases, the band observed at 3740 cm^{-1} and related to silanol groups is not perturbed by adsorbed pyridine, since these OH groups do not present an acid character.

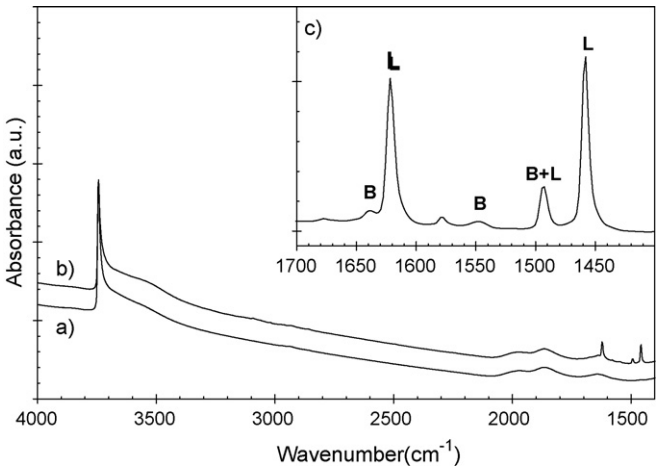

Fig. 2. Typical FTIR spectra, mass corrected, for Ga-MCM-41 materials. Spectra acquired before (a) and after pyridine adsorption-outgassing at 150 °C (b), and detail of the corresponding difference spectra (c), with band assignments. B, Brønsted sites; L, Lewis sites.

It is expected that the number of acid sites present at the surface of the Ga-MCM-41 materials will follow the order of decreasing Si/Ga ratio (increasing concentration of Ga). Nevertheless, Ga-MCM-41 materials obtained by the standard direct synthesis procedure (series GaM*R*) presented a rather irregular variation of Lewis acidity with bulk Si/Ga ratio. When combining the direct synthesis method with extended template removal procedures and longer calcination times (series GaM*R*X), the overall acidity of the materials is increased and follows the order of decreasing Si/Ga ratios. Ga-MCM-41 materials prepared by impregnation of Si-MCM-41 with gallium nitrate (series GaM*R*I) also follow the expected acidity trend. These results suggest that incomplete template removal may have occurred for series GaM*R*, thus blocking up the access of pyridine molecules to acid sites present in the surface and diminishing their chemical effects.

From Table 4 it is clear that the main fraction of the acid sites detected in the prepared Ga-MCM-41 is Lewis sites (over 90%). As the outgassing temperature rises from 150 to 300 °C, the gallosilicates keep 55–68% of the amount of pyridine adsorbed in the Lewis sites. Therefore, most of these sites can be considered to be strong acid sites. On the other hand, Brønsted sites are present in much lower concentrations than Lewis sites. For series GaM*R*, Brønsted sites are barely detectable, while for series GaM*R*X and GaM*R*I these sites are responsible for only ~6% and ~8% of the total amount of pyridine adsorbed. Nevertheless, at 300 °C pyridine associated to Brønsted sites is not observed in the spectra for both the materials analysed. Accordingly, the Brønsted acid sites present in the Ga-MCM-41s can be considered as weak acid sites.

3.4. Preparation of the supported catalysts

Modification of Al-MCM-41 supports, by pre-treatment with MAO, prior to zirconocene immobilisation, reduces the influence of framework acidity on polymerisation behaviour [2,31]. This way, in the present study, only the direct immobilisation method was employed to prepare the supported catalysts. It is known that aluminium present in Al-MCM-41 improves the retention of the

Table 3
Catalysts prepared and activities obtained in the polymerisation of ethylene.

Support	Bulk Si/Ga	Zr contents in support (μmol/g)	Polymerisation activities (kg/(mol$_{Zr}$ h))	
			$Al_{MAO}/Zr = 500$	$Al_{MAO}/Zr = 1500$
None	–	(a)	>5000	–
Si-MCM-41	∞	13	310	830
GaM139	139	50	1260	2210
GaM116	116		1660	2700
GaM82	82		1030	1790
GaM63	63		1320	2590
GaM47	47		400	1060
GaM82X[a]	82	50	1100	3030
GaM63X[a]	63		1030	1970
GaM47X[a]	47		560	920
GaM150I	150	50	790	1290
GaM126I	126		1340	2190
GaM83I	83		890	1250

(a) Solution polymerisation, 1 μmol Zr in reactor.
[a] Extended treatment for template removal.

metallocene in the siliceous support in a direct impregnation, when compared to Si-MCM-41 [2,31]. As discussed above, XPS data (Table 2) report surface compositions with much lower Ga concentrations than expected from the bulk composition of the Ga-MCM-41 materials. Nevertheless, for any of the supports, the very low Ga loadings proved to be enough to immobilise at least four times more metallocene than Si-MCM-41 did. Gallium seems to be as effective as aluminium (if not better) in creating a surface able to capture the metallocene.

3.5. Study of ethylene polymerisation behaviour

A previous communication highlighted that zirconocene dichloride could be efficiently supported over Ga-containing MCM-41 materials, producing supported catalysts with high activities over mild polymerisation conditions [25]. In this paper, the study is expanded to a greater number of supports, prepared according to distinct procedures. The three sets of Ga-MCM-41 supports prepared present surfaces with different "chemical properties", in terms of chemical composition, Ga segregation effects and acidity properties, while keeping the same general structural characteristics, as demonstrated by the results discussed thus far. The influence of these "chemical properties", over polymerisation activity is discussed in the present section.

Table 3 presents the catalysts prepared and the corresponding polymerisation activities, using Al_{MAO}/Zr ratios equal to 500 and 1500. For comparison, previous results from solution polymerisation and Si-MCM-41 are also included [31]. The activity values obtained with Cp_2ZrCl_2/Ga-MCM-41 systems for Al/Zr = 500 represent around 30% of the activity obtained in solution, which can be considered a very good result [25]. A preliminary characterisation of polyethylene samples obtained from these supported systems by DSC technique showed an increase in the melting temperature of about 1 °C relatively to the non-supported system. Accordingly a slight increase of the average molecular weight may be expected for the supported systems when compared to the value obtained in the corresponding homogeneous conditions ($M_w = 4 \times 10^5$ g/mol).

3.5.1. Relation with support chemical composition

The dependence of polymerisation activity on the XPS and bulk Si/Ga ratio is shown in Figs. 3 and 4. According to structural data presented in the previous sections, Ga-MCM-41 support particles provide, besides its external surface area, a high porous volume and internal surface area for metallocene binding and activation and consequent polymer formation. Therefore both bulk and external chemical compositions are expected to contribute individually to the overall polymerisation activity: if polymer formation occurs predominantly at the external surface of the mesoporous gallosilicates, activity should correlate to Si/Ga ratios assessed by XPS; on the contrary, if polymer formation at external surface can be neglected relatively to the total amount of polymer formed, bulk Si/Ga ratio should correlate better.

Data from Fig. 3 show rather dispersed sets of points that do not seem to follow a specific trend. When looking to Fig. 4, more defined trends are apparent; activity increases with bulk Si/Ga ratio up to a maximum value and then decreases. However, bulk Si/Ga is not the only parameter determining activity and other factors influence the overall activity. In particular, at identical bulk Si/Ga ratios, impregnated supports led to lower polymerisation activities compared to

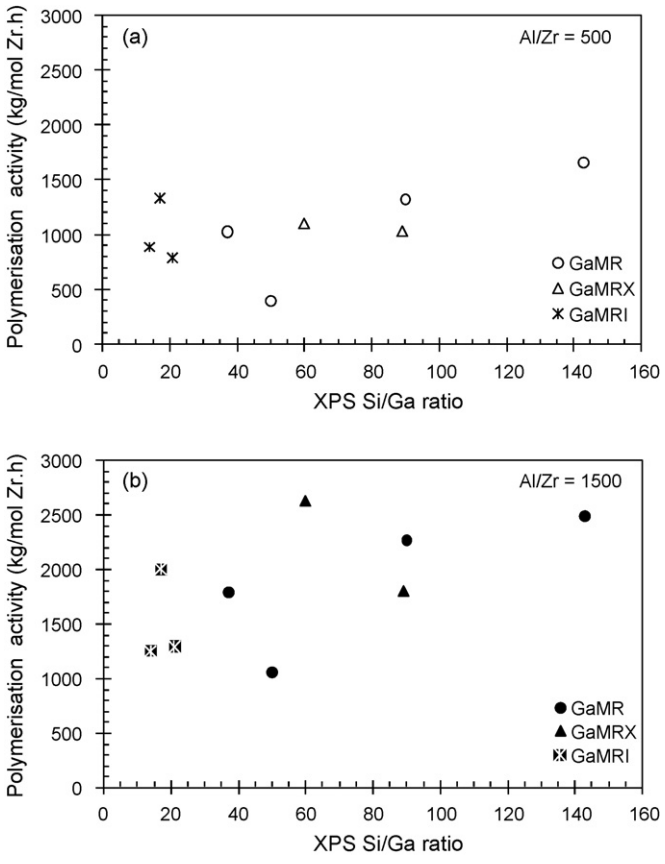

Fig. 3. Polymerisation activities for (a) Al/Zr = 500 and (b) Al/Zr = 1500 plotted as function of XPS Si/Ga ratios.

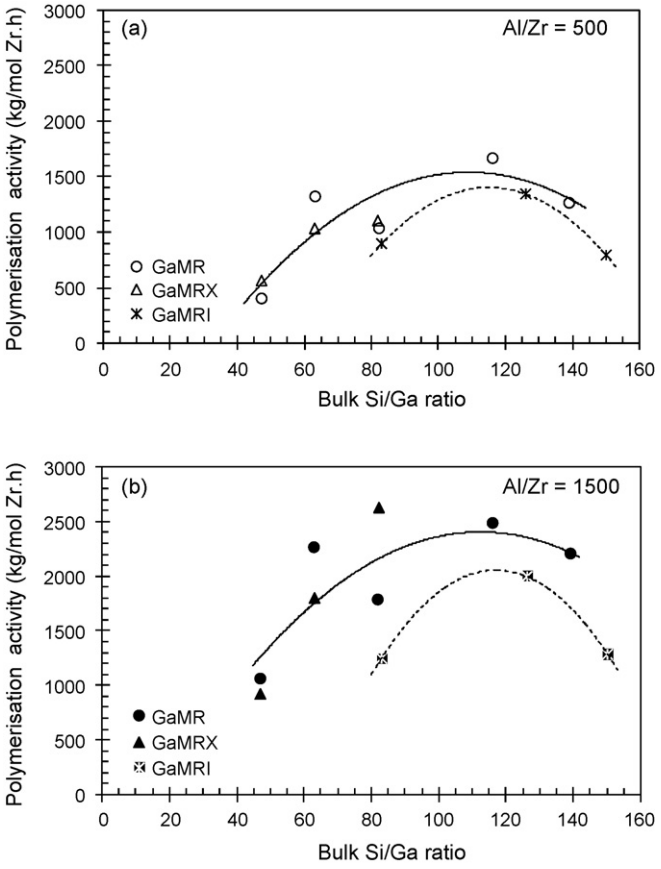

Fig. 4. Polymerisation activities for (a) Al/Zr = 500 and (b) Al/Zr = 1500 plotted as function of bulk Si/Ga ratios.

direct synthesis ones. This result may be tentatively interpreted on the basis of the much higher segregation effect occurring in the impregnated samples (which exhibit external Ga loads roughly eight times higher than the bulk Ga compositions) when compared with direct synthesis supports. In that case very high Ga segregation will be reflected negatively on polymerisation activity. One explanation could be the formation of Ga aggregates on the particle surface of impregnated samples with low XPS Si/Ga ratio, although no crystalline aggregates of gallium oxide or other gallium phases were detected by X-ray diffraction.

3.5.2. Relation with support surface acidity characteristics

As pointed out before, differences on synthesis and template removal procedures affect not only chemical composition and Ga segregation, but also induce significant changes on the overall acidic properties of the support (type, number and strength of acid sites). It is known that the acidic properties of supports may influence the type of interaction with the metallocene complex and its activation process, with consequent effects on overall productivity. The relation between the polymerisation activity and the surface acidity characteristics of the support will be now analysed, on the basis of the models proposed in published literature that explain the interaction of methylated metallocenes with silica–alumina and alumina [16–18].

One common feature in these models is the generation of cationic, "cationic-like" or polarised species when one of the labile ligands in the methylated metallocene is captured by the Lewis acidic aluminium present in the surface. On the other hand, weak Brønsted sites would be responsible for the displacement of the ligands in the metallocene, converting it to inactive species containing μ-oxo Zr–O–Si structures. Strong Brønsted sites, in some less frequent cases, have been proposed to ionize with delocalisation of the resulting negative charge but do not produce inactive μ-oxo structures.

Scheme 1 represents an adaptation of the above-described models to the case of the interaction of zirconocene dichloride (Cp_2ZrCl_2) with the acid sites known for zeolites and zeolite-like mesoporous aluminosilicates. Weak Brønsted sites lead to μ-oxo species with a small charge separation in the Zr–O bond, which however is not enough to originate the cationic active species. With stronger Brønsted sites, negative charge delocalisation withdraws electronic density from the μ-oxo bond, creating a much more polarised species. Although none of the species represented in Scheme 1 is active by itself, it was already proposed that μ-oxo species may be activated in presence of MAO [19], explaining the low polymerisation activity levels obtained for pure silica supports. In the present model it is proposed that neutral and slightly polarised μ-oxo complexes, issued from weak Brønsted sites, are less prone to be converted to active species, than the cationic or strongly polarised species, formed on Lewis or strong Brønsted sites. According to this scheme, and depending on the nature and strength of the existing acid sites of the support, the activation of the metallocene and the corresponding formation of the active species can be favoured or hindered.

As mentioned previously, many of the Ga-MCM-41 samples present weak Brønsted sites. Therefore a negative effect on activity is expected. On the other hand, a positive effect on activity is expected for Ga-MCM-41 samples exhibiting increased number of Lewis centres and acidity strengths. In a rather simplified picture, the polymerisation activity of catalysts prepared from supports containing both Lewis acid sites and weak Brønsted acid sites will be affected by two opposite effects. Accordingly, the polymerisation activity observed when using these mesoporous gallosilicates is expected to increase with the fraction of "strong" Lewis sites present in these mesoporous gallosilicates.

The dependence of polymerisation activity on the fraction of Lewis sites (ratio between number of Lewis sites and total number of acid sites, according to data reported in Table 4) is shown in Fig. 5 and seems to follow the expected trend. Maximal activity is obtained for samples without Brønsted acidity, and very small amounts of weak Brønsted sites (less than 10%) lead to a severe reduction of activity. This drastic effect can also be seen in Fig. 6, representing the polymerisation activity as a function of total concentration of weak Brønsted sites.

When using non-methylated zirconocene dichloride (Cp_2ZrCl_2), even if the acidity characteristics of support enable the abstraction of a chloride ligand and the formation of a cationic species, it will be necessary to further alkylate this species in order to obtain the active species (Cp_2ZrR^+). If no MAO or other alkylat-

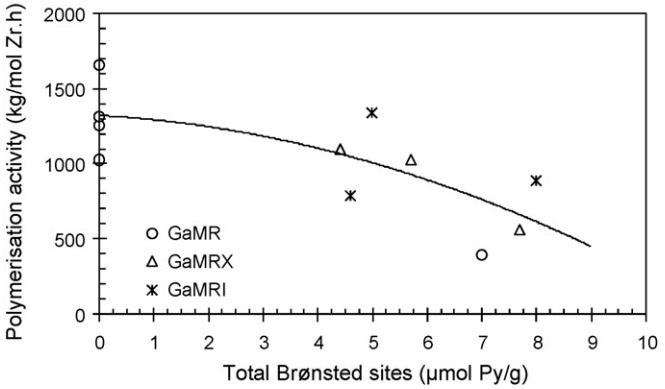

Fig. 5. Polymerisation activities (for $Al_{MAO}/Zr \sim 500$) plotted as function of the fraction of Lewis sites (as measured with pyridine at 150 °C).

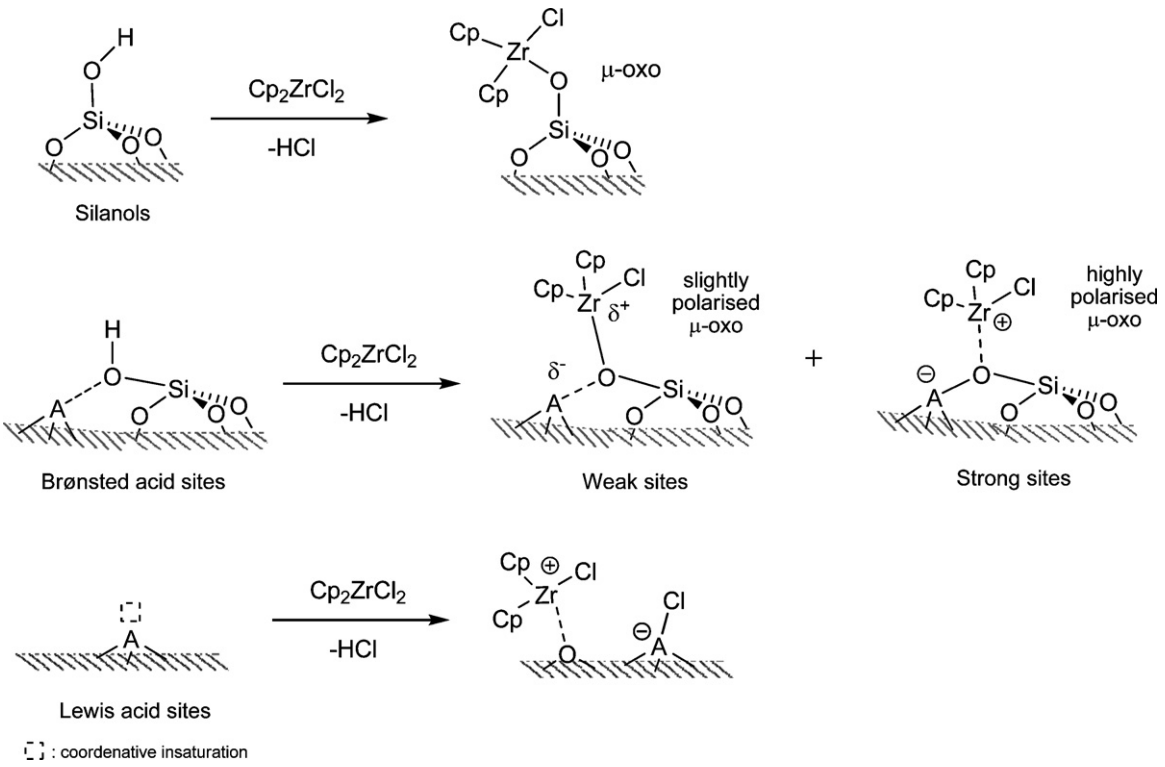

Scheme 1. Models for the interactions of metallocene Cp_2ZrCl_2 with species present in acidic silicate surfaces (A: acidic element).

Table 4
Amounts of pyridine adsorbed for each type of acid site, as measured by FTIR.

Sample type	Sample	Bulk Si/Ga	Pyridine adsorbed (μmol/g Ga-MCM-41)			
			150 °C (total sites)		300 °C (strong sites only)	
			Lewis sites	Brønsted sites	Lewis sites	Brønsted sites
Ga-MCM-41 by direct synthesis	GaM139	139	65	0	36	0
	GaM116	116	53	0	36	0
	GaM82	82	31	0	19	0
	GaM63	63	13	0	3.4	0
	GaM47	47	93	7.0	59	0
	GaM82X[a]	82	88	4.4	55	0
	GaM63X[a]	63	97	5.7	60	0
	GaM47X[a]	47	127	7.7	79	0
Ga-MCM-41 by impregnation of Si-MCM-41	GaM150I	150	52	4.6	26	0
	GaM126I	126	66	5.0	38	0
	GaM83I	83	92	8.0	54	0

[a] Extended treatment for template removal.

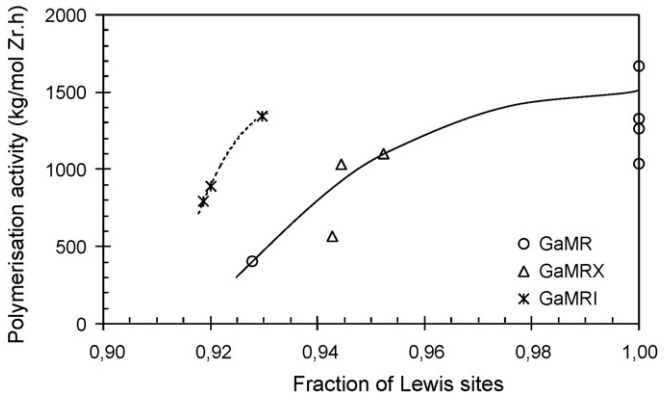

Fig. 6. Polymerisation activities (for $Al_{MAO}/Zr \sim 500$) plotted as function of the total concentration of Brønsted sites (as measured with pyridine at 150 °C).

ing agent is added during polymerisation, the active species cannot be formed and therefore no activity is observed. In order to confirm that Ga-MCM-41 materials can indeed promote the formation of the cationic precursor of the active species, some polymerisation experiments were performed using TIBA in place of MAO and $Al_{TIBA}/Zr \sim 50$. Indeed, after 2 h, polyethylene is recovered from the reactor mixture. This supports the assumption that mesoporous materials containing acidic Ga are able to polarise the Zr–Cl bond in the metallocene and produce cationic metallocenium ions, or cationic-like analogues that after alkylation by TIBA form the active species, which are able to promote the polymerisation of ethylene.

The interpretation here presented although showing a correlation between polymerisation activity and support acidity is a very simplified picture of reality. In fact the type, number and strength of the acid sites cannot be varied separately, leading to a very complex system of interactions with opposite effects on polymerisation activity. Moreover, we must keep in mind the possible role that non-

acidic SiOH groups may play in polymerisation activity, since vicinal silanol groups may lead to irreversible deactivation of Cp_2ZrCl_2 during the immobilisation procedure. Although in the present study all the mesoporous solids were dried prior to impregnation using the same conditions, at the present state of the investigation we cannot exclude that differences may exist on the amount and type of surface silanol groups. Further studies are in progress, aiming to clarify this aspect.

4. Conclusion

A series of Ga-MCM-41 materials, prepared using well-established procedures, was used to assemble a large set of metallocene catalyst supports. The different synthesis and template removal procedures used in the preparation of these supports do not affect significantly its structural parameters. However, they result in different surface characteristics in terms of chemical composition, segregation effects and surface acidity properties with important effects on final polymerisation activity. XPS experiments demonstrated that the Ga distribution is strongly dependent on the synthesis procedure (direct synthesis or impregnation) and also, in some extent, on the thermal treatment used for the template removal. Careful characterisation of the structural features and chemical properties of the supports prepared was of paramount importance to assure that, as far as possible, all effects are accounted for when explaining the catalytic performance.

The present work corroborates other studies pointing out to the important role that acidity properties of the support may play on the metallocene activation process. It has been shown that polymerisation activities depend on the balance between Lewis acid sites, which favour the formation of active species, and weak Brønsted sites forming μ-oxo species less prone to activation.

Acknowledgments

The authors are grateful for the funding of this work by the Fundação para a Ciência e a Tecnologia (FCT), under project PDCT/CTM/66408/2006. J.M.C. thanks the FCT for his PhD scholarship (ref. SFRH/BD/16547/2004). Financial support by FCT, for acquisition of XRD equipment, under project CONC-REEQ/700/2001, is also gratefully acknowledged.

References

[1] Y.S. Ko, T.K. Han, J.W. Park, S.I. Woo, Macromol. Rapid Commun. 17 (1996) 749–758.
[2] H. Rahiala, I. Beurroies, T. Eklund, K. Hakala, R. Gougeon, P. Trens, J.B. Rosenholm, J. Catal. 188 (1999) 14.
[3] K.S. Lee, C.G. Oh, J.H. Yim, S.K. Ihm, J. Mol. Catal. A: Chem. 159 (2000) 301.
[4] B.M. Weckhuysen, R.R. Rao, J. Pelgrims, R.A. Schoonheydt, P. Bodart, G. Debras, O. Collart, P. Van Der Voort, E.F. Vansant, Chem. Eur. J. 6 (2000) 2960.
[5] I.S. Paulino, U. Schuchardt, Catal. Commun. 5 (2004) 5.
[6] X.C. Dong, L. Wang, G.H. Jiang, Z.R. Zhao, T.X. Sun, H.J. Yu, W.Q. Wang, J. Mol. Catal. A: Chem. 240 (2005) 239–244.
[7] C. Guo, D. Zhang, F.S. Wang, G.X. Jin, J. Catal. 234 (2005) 356–363.
[8] K. Kageyama, J. Tamazawa, T. Aida, Science 285 (1999) 2113.
[9] Z.B. Ye, S.P. Zhu, W.J. Wang, H. Alsyouri, Y.S. Lin, J. Polym. Sci., Part B: Polym. Phys. 41 (2003) 2433.
[10] M. Alexandre, E. Martin, P. Dubois, M. Garcia-Marti, R. Jerome, Macromol. Rapid Commun. 21 (2000) 931–936.
[11] J. He, X. Duan, D.G. Evans, R.F. Howe, J. Porous Mater. 9 (2002) 49–56.
[12] P. Dubois, M. Alexandre, R. Jerome, Macromol. Symp. 194 (2003) 13–26.
[13] H. Nakajima, K. Yamada, Y. Iseki, S. Hosoda, A. Hanai, Y. Oumi, T. Teranish, T. Sano, J. Polym. Sci., Part B: Polym. Phys. 41 (2003) 3324.
[14] H. Kosslick, G. Lischke, G. Walther, W. Storek, A. Martin, R. Fricke, Micropor. Mater. 9 (1997) 13–33.
[15] A. Tuel, S. Gontier, Chem. Mater. 8 (1996) 114–122.
[16] C. Coperet, M. Chabanas, R.P. Saint-Arroman, J.M. Basset, Angew. Chem. Int. Ed. 42 (2003) 156–181.
[17] M. Jezequel, V. Dufaud, M.J. Ruiz-Garcia, F. Carrillo-Hermosilla, U. Neugebauer, G.P. Niccolai, F. Lefebvre, F. Bayard, J. Corker, S. Fiddy, J. Evans, J.P. Broyer, J. Malinge, J.M. Basset, J. Am. Chem. Soc. 123 (2001) 3520–3540.
[18] T.J. Marks, Acc. Chem. Res. 25 (1992) 57–65.
[19] C. Alonso, A. Antinolo, F. Carrillo-Hermosilla, P. Carrion, A. Otero, J. Sancho, E. Villasenor, J. Mol. Catal. A: Chem. 220 (2004) 285–295.
[20] V.I. Costa Vayá, P.G. Belelli, J.H.Z. dos Santos, M.L. Ferreira, D.E. Damiani, J. Catal. 204 (2001) 1–10.
[21] T. Sano, T. Niimi, T. Miyazaki, S. Tsubaki, Y. Oumi, T. Uozumi, Catal. Lett. 71 (2001) 105.
[22] T. Miyazaki, Y. Oumi, T. Uozumi, H. Nakajima, S. Hosoda, T. Sano, Stud. Surf. Sci. Catal. 142 (2002) 871–878.
[23] T. Sano, Y. Oumi, Cat. Surv. Asia 8 (2004) 295–304.
[24] C. Covarrubias, R. Quijada, R. Rojas, Appl. Catal. A 347 (2008) 223–233.
[25] J.M. Campos, J.P. Lourenco, A. Fernandes, M.R. Ribeiro, Catal. Commun. 10 (2008) 71–73.
[26] J.M. Kim, S. Jun, R. Ryoo, J. Phys. Chem. B 103 (1999) 6200–6205.
[27] B. Lindlar, A. Kogelbauer, P.J. Kooyman, R. Prins, Micropor. Mesopor. Mater. 44 (2001) 89–94.
[28] N. Lang, P. Delichere, A. Tuel, Micropor. Mesopor. Mater. 56 (2002) 203–217.
[29] P. Oliveira, A. Machado, A.M. Ramos, I.M. Fonseca, F.M.B. Fernandes, A.M.B. Do Rego, J. Vital, Catal. Commun. 8 (9) (2007) 1366–1372.
[30] C.A. Emeis, J. Catal. 141 (1993) 347–354.
[31] J.M. Campos, M.R. Ribeiro, J.P. Lourenco, A. Fernandes, J. Mol. Catal. A: Chem. 277 (2007) 93–101.
[32] J.P. Lourenço, A. Fernandes, C. Henriques, M.F. Ribeiro, Micropor. Mesopor. Mater. 94 (2006) 56–65.